European Journal of Medicinal Chemistry 92 (2015) 799–806

Contents lists available at ScienceDirect

European Journal of Medicinal Chemistry

journal homepage: http://www.elsevier.com/locate/ejmech

Original article

Potent acetylcholinesterase inhibitors: Design, synthesis, biological evaluation, and docking study of acridone linked to 1,2,3-triazole derivatives

Maryam Mohammadi-Khanaposhtani [a], Mina Saeedi [b], Narges Shamsaei Zafarghandi [a], Mohammad Mahdavi [c], Reyhaneh Sabourian [d], Elahe Karimpour Razkenari [d], Heshmatollah Alinezhad [e], Mahnaz Khanavi [f], Alireza Foroumadi [c], Abbas Shafiee [c], Tahmineh Akbarzadeh [a, d, *]

[a] Department of Medicinal Chemistry, Faculty of Pharmacy, Tehran University of Medical Sciences, Tehran 14176, Iran
[b] Medicinal Plants Research Center, Tehran University of Medical Sciences, Tehran, Iran
[c] Department of Medicinal Chemistry, Faculty of Pharmacy and Pharmaceutical Sciences Research Center, Tehran University of Medical Sciences, Tehran 14176, Iran
[d] Persian Medicine and Pharmacy Research Center, Tehran University of Medical Sciences, Tehran, Iran
[e] Faculty of Chemistry, University of Mazandaran, Babolsar, Iran
[f] Department of Pharmacognosy, Tehran University of Medical Sciences, Tehran 14176, Iran

ARTICLE INFO

Article history:
Received 23 September 2014
Received in revised form
20 January 2015
Accepted 21 January 2015
Available online 22 January 2015

Keywords:
Alzheimer's disease
Acetylcholinesterase
Acridone-1,2,3-triazole
Docking study

ABSTRACT

A novel series of acridone linked to 1,2,3-triazole derivatives have been synthesized and evaluated *in vitro* for their acetylcholinesterase (AChE) and butyrylcholinesterase (BChE) inhibitory activities. The synthetic approach was started from the reaction of 2-bromobenzoic acid with aniline derivatives and subsequent cyclization reaction to give acridone derivatives. Then, reaction of the later compounds with propargyl bromide followed by azide–alkyne cycloaddition reaction (click reaction) led to the formation of the title compounds in good yields. Among the synthesized compounds, 10-((1-(4-chlorobenzyl)-1*H*-1,2,3-triazol-4-yl)methyl)-2-methoxyacridin-9(10*H*)-one **9g**, depicted the most potent anti-AChE activity (IC_{50} = 7.31 μM). Also, docking study confirmed the results obtained through *in vitro* experiments and predicted possible binding conformation.

1. Introduction

Alzheimer's disease (AD) is the most common neurodegenerative syndrome, recognized as the origin of dementia among older people in which cognitive characteristics such as intelligence, memory, language, and speech are overshadowed [1,2]. The number of people affected by AD is estimated to triple by 2050 along with severe economic detriment [3]. The rapid growth of AD as well as medical and social issues in both developed and developing countries has attracted the attention of medicinal chemists to develop their drug discovery investigations in this area [4].

The pathogenic background of AD is not comprehensively perceived and it seems that cholinergic system disorders, accelerated aggregation of β-amyloid peptides and the dyshomeostasis of biometals are the most common factors involved in AD [5–9]. It has been revealed that most of AD symptoms are caused by acetylcholine-producing system dysfunction through AChE/BChE-catalyzed hydrolysis of acetylcholine [10,11]. In spite of the fact that physiological function of AChE in neuromuscular junction is well-documented, the function of BChE has not been fully recognized. Carson et al. demonstrated that the activity of both AChE and BChE is related to masses of tangled paired helical filaments in neurons with NFT [12].

Although a wide range of research programs has focused on developing AChE inhibitors, therapeutic drugs on the market are not so much available since their efficacy is limited to various adverse effects. In this context, four commonly prescribing AChE inhibitors including tacrine, donepezil, rivastigmine, and

* Corresponding author. Department of Medicinal Chemistry, Faculty of Pharmacy, Tehran University of Medical Sciences, Tehran 14176, Iran.
E-mail address: akbarzad@tums.ac.ir (T. Akbarzadeh).

http://dx.doi.org/10.1016/j.ejmech.2015.01.044
0223-5234/

galantamine have been approved by the European and United States regulatory authorities [13].

Success of tetrahydroacridine derivatives particularly tacrine, as the first centrally-acting AChEI approved for the treatment of AD, led researchers to develop novel acridine based agents to reduce the side effects [14–16]. At this juncture, acridones absorbed our attention as some naturally occurring derivatives exhibited AChE inhibitory activity [17]. Comprehensive literature review exhibited that the effectiveness of synthetic acridones in the treatment of AD have not been fully investigated. Indeed, brilliant previous record of 1,2,3-triazole subunit in inhibition of AChE [18–20] and our experiences in the synthesis of anti-acetylcholinesterase agents [21–23] encouraged us to design and evaluate novel acridone linked to 1,2,3-triazole scaffold against AChE and BChE (Scheme 1).

2. Results and discussion

2.1. Chemistry

The synthetic route for the synthesis of acridone linked to 1,2,3-triazoles **9** has been depicted in Scheme 1. It was started from the Ullmann condensation reaction of 2-bromobenzoic acid **1** and various aniline derivatives **2** [24] in the presence of potassium carbonate and copper in EtOH at reflux to give 2-arylamino benzoic acids **3**. They easily underwent cyclization reaction in the presence of PPA at 100 °C and afforded acridone derivatives **4** [25]. Acridone derivatives **4** reacted with propargyl bromide **5** using potassium *tert*-butoxide in DMSO at room temperature. The resulting 10-(prop-2-yn-1-yl)acridin-9-one derivatives **6** were prone to be participated in click reaction through the method described by Sharpless et al. to construct 1,2,3-triazole ring [26]. Accordingly, different benzyl chloride derivative **7** and sodium azide reacted in the presence of Et_3N in the mixture of H_2O/*t*-BuOH at room temperature. Then, mixture of 10-(prop-2-yn-1-yl)acridin-9-one derivative **6** and CuI was added to the freshly prepared azide derivative **8** and the reaction was continued at room temperature for 24–56 h to give the corresponding products **9** in good yields (73–89%).

2.2. Pharmacology

2.2.1. Inhibitory activity against AChE and BChE

The *in vitro* activity of the all compounds **9a**–**n** was evaluated for their ability to inhibit AChE and BChE by Ellman's method and compared with rivastigmine as the reference drug [27] (Table 1). All data were presented as mean ± S.E. of three independent experiments.

Based on the IC_{50} values for AChE, most of the synthesized compounds exhibited satisfactory inhibitory activity in the range of sub-micromolar concentrations (IC_{50} values of 7.31–88.10 μM) comparing with rivastigmine as the reference drug. As can be seen in Table 1, compounds **9d**–**g**, **9l**, and **9n** were found to be more

Table 1
The IC_{50} values of the compounds **9** against AChE and BChE.[a]

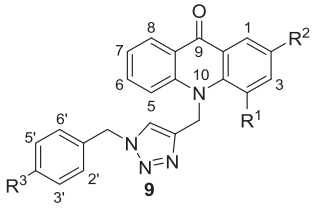

Entry	Compound **9**	R^1	R^2	R^3	AChE inhibition [IC_{50} (μM/ml)]	BChE inhibition [IC_{50} (μM/ml)]
1	**9a**	H	H	H	≥100	≥100
2	**9b**	H	H	Cl	59.68 ± 0.01	≥100
3	**9c**	H	Cl	H	88.10 ± 0.03	≥100
4	**9d**	H	Cl	Cl	17.69 ± 0.52	≥100
5	**9e**	H	Cl	NO_2	38.33 ± 0.04	≥100
6	**9f**	H	OMe	H	23.99 ± 0.01	≥100
7	**9g**	H	OMe	Cl	7.31 ± 0.03	≥100
8	**9h**	H	Br	H	68.06 ± 0.01	≥100
9	**9i**	H	Br	Cl	45.57 ± 0.04	≥100
10	**9j**	H	Br	NO_2	52.82 ± 0.02	≥100
11	**9k**	H	Me	H	≥100	≥100
12	**9l**	H	Me	Cl	10.84 ± 0.07	87.17 ± 1.00
13	**9m**	F	H	H	≥100	≥100
14	**9n**	F	H	Cl	24.53 ± 0.02	≥100
15	**Rivastigmine**				11.07 ± 0.01	N.d

[a] Data are expressed as Mean ± SE (three independent experiments).

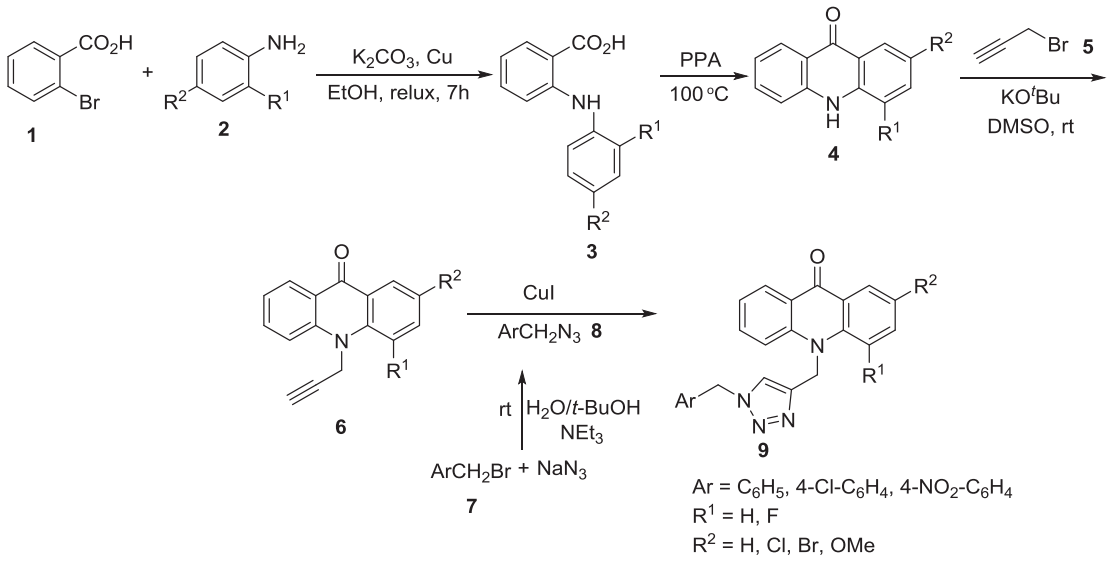

Scheme 1. Synthesis of acridone linked to 1,2,3-triazole derivatives **9**.

potent anti-AChE and among them, **9g** was the most potent compound (IC_{50} = 7.31 μM) in comparison to rivastigmine (IC_{50} = 11.07 μM). It is notable that compound **9l** (IC_{50} = 10.84 μM) depicted similar activity regarding with reference drug.

The results showed that the electronic properties of substituents both on acridone and 1,2,3-triazole rings affect anti-AChE activity since no activity was observed for compound **9a**. It was found that the presence of 4-substituted chlorine on the pendant benzyl group plays significant role in anti-AChE activity and it is truly confirmed by the obtained results for compounds **9b**, **9d**, **9g**, **9i**, **9l**, and **9n**. Introduction of strong electron-withdrawing group (NO_2) into the pendant benzyl group instead of chlorine in compounds **9e** and **9j** decreased activity comparing with compounds **9d** and **9i**, respectively.

It seems that the presence of any groups instead of hydrogen on the 2-substituted acridon moieties led to the increase of inhibitory activity and it is demonstrated in compounds **9b**, **9d**, **9g**, **9i**, and **9l** in the order of OMe > Me ≥ Cl > Br. It is worthwhile mentioning that introduction of fluorine group into 4-position of acridone ring enhanced the activity more than two-fold and it is clearly observed in compound **9n** versus compound **9b**. The effect of substituents on the pendant benzyl group was perceived to be more effective and clearly synergistic effect of this group and substituents on the acridone ring would be observed.

Finally, the obtained result related to compound **9g** as the best candidate of the anti-AChE is in good agreement with those reported in the literature [28,29]. The efficiency of methoxy and chlorine groups to create useful interactions with the active site of enzyme, plays crucial role in the inhibitory activity. As reported in the literature [28], formation of a hydrogen bond between oxygen of OMe and that hydrogen belongs to OH of amino acid is expected. Also, a weak interaction between chlorine and backbone carbonyl group of amino acid is beneficial [29].

Altogether, all synthesized products except compound **9l** showed no BChE inhibition (IC_{50} > 100 μM) and it was remarkably lower than AChE inhibitory activity.

2.2.2. 1,1-Diphenyl-2-picrylhydrazyl (DPPH) radical scavenging activity

1,1-Diphenyl-2-picrylhydrazyl radical scavenging activity (DPPH) assay was utilized to determine the total antioxidant activity of the compounds **9b**, **9c**, **9f**, **9k**, and **9m** based on the method described in the literature [30]. All results are shown in Table 2. In this colorimetric method, 1,1-diphenyl-2-picrylhydrazyl radical has an absorption band at 515 nm which is disappeared upon reduction by an antioxidant agent. The inhibition percentage values were determined by comparison to butylated hydroxyanisole (BHA) as a standard antioxidant. The above mentioned compounds showed no significant antioxidant activities.

2.2.3. Docking studies

During our investigations, we applied docking studies parallel to the synthesis and evaluation of compounds **9** to obtain scrutinized concept on the interactions and binding to the active sites of AChE and the related inhibitory activities. Our results are shown in Figs. 1–3 which were performed with the most active compound **9g** using Autodock Tools (1.5.6), discovery studio 4.0 client, and Chemira 1.9 software (UCFS package). Several ligand-bounded crystallographic structures of AChE are available in the RCSB protein data bank (http://www.rcsb.org/pdb/home/home.do). Herein, PDB structure of 1EVE was retrieved for docking purpose.

As expected, planar structure of acridone and 1,2,3-triazole in compound **9g** led to the important interactions which was confirmed with docking study (Fig. 1). It revealed that there is an important interaction with catalytic anionic site (CAS) in which two amino acids Phe330 and Trp84 are responsible for the corresponding interactions. Phe330 is responsible for binding the 1,2,3-triazole part in the synthesized inhibitor **9g** with π–π interactions. Also, Trp84 possessing aromatic moiety is involved in π–π interaction of acridone moiety. As can be seen in Fig. 2, it seemed that the presence of chlorine on the pendant benzyl group led to the formation of weak interaction with backbone carbonyl group which is beneficial interaction [29]. As the best result was obtained for the compound **9g** possessing methoxy group at 2-position of acridone moiety, docking study was dedicated for the possible interaction of methoxy group. According to Fig. 3, it is clear that a hydrogen bond can be formed between oxygen of OMe and that hydrogen belongs to OH of Ser122 [28].

2.2.4. Screening of pharmacokinetic properties

To gain insight into aspects of the pharmacokinetic properties of synthesized compounds **9a**–**n**, some of their physicochemical and topological properties including a number of H-bond donors (HBD), a number of H-bond acceptors (HBA), octanol–water partition coefficients (Clog *P*), the polar surface area (tPSA), and a number of rotatable bonds (RBC) were calculated and shown in Table 3. According to Lipinski rule of 5 [31,32], most compounds were found to be a likely orally active drug in humans and MW ≤ 500, HBD ≤ 5, HBA ≤ 10 and Clog *P* ≤ 5 were reported. The molecular weight of compounds was between 366.42 and 490.31 Da, their Clog *P* was in the range of 3.83–5.27. They had 0 H-bond donors and 4-6 H-bond acceptors. Also, they possessed tPSA between 48.27–100.08 and 4–5 RBC. The obtained results revealed that prepared acridone linked to 1,2,3-triazoles **9** would have satisfactory pharmacokinetics: solubility and permeability after the oral admission as drug

Table 2
DPPH antioxidant activities of the compounds **9b**, **9c**, **9f**, **9k**, and **9m**.[a]

Entry	Compound **9**	Inhibition (%) (700 μg/ml)	EC_{50} (μg/ml)
1	**9b**	21.78 ± 0.22	>333
2	**9c**	26.60 ± 0.08	>700
3	**9f**	8.65 ± 0.45	>700
4	**9k**	7.09 ± 0.84	>333
5	**9m**	14.79 ± 0.98	>700
6	**BHA**	96.69 ± 0.53	–

[a] Data are expressed as Mean ± SE (three independent experiments).

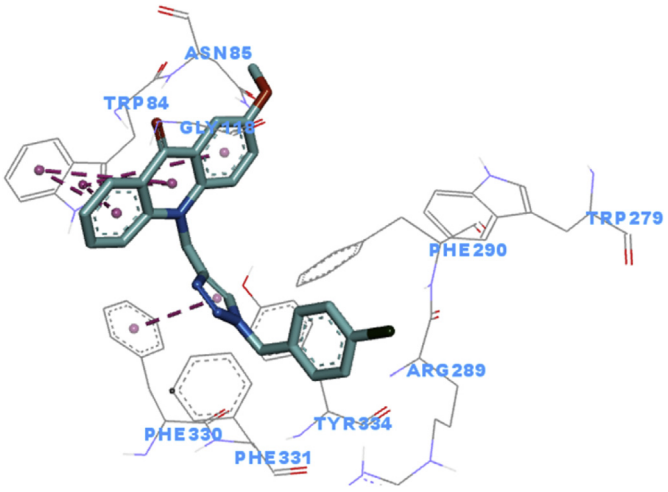

Fig. 1. The most active compound **9g** in the active site of AChE enzyme. The probable π–π stacking interaction of acridone and 1,2,3-triazole rings whit Trp84 and Phe330, respectively. They are shown by dashed line.

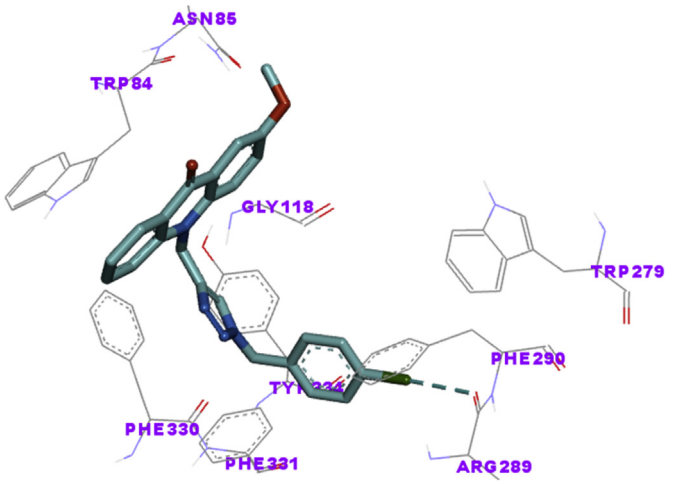

Fig. 2. Interaction of chlorine and Arg289 in compound **9g**.

Table 3
Molecular descriptors[a] of compounds **9**.

Entry	Compound **9**	HBD	HBA	Clog *P*	tPSA [Å^2]	MW	RBC
1	**9a**	0	4	3.83	48.27	366.42	4
2	**9b**	0	4	4.54	48.27	400.11	4
3	**9c**	0	4	4.56	48.27	400.66	4
4	**9d**	0	4	5.27	48.27	435.31	4
5	**9e**	0	6	4.3	100.08	445.09	5
6	**9f**	0	5	3.92	57.5	396.31	5
7	**9g**	0	5	4.63	57.5	430.89	5
8	**9h**	0	4	4.71	48.27	445.21	4
9	**9i**	0	4	5.42	48.27	479.71	4
10	**9j**	0	6	4.45	100.08	490.31	5
11	**9k**	0	4	4.33	48.27	380.16	4
12	**9l**	0	4	5.04	48.27	414.89	4
13	**9m**	0	4	3.99	48.27	384.14	4
14	**9n**	0	4	4.77	48.27	366.42	4

[a] HBD: a number of H-bond donors, HBA: a number of H-bond acceptors, Clog *P*: the octanol–water partition coefficient, tPSA: the polar surface area, RBC: a number of rotatable bonds.

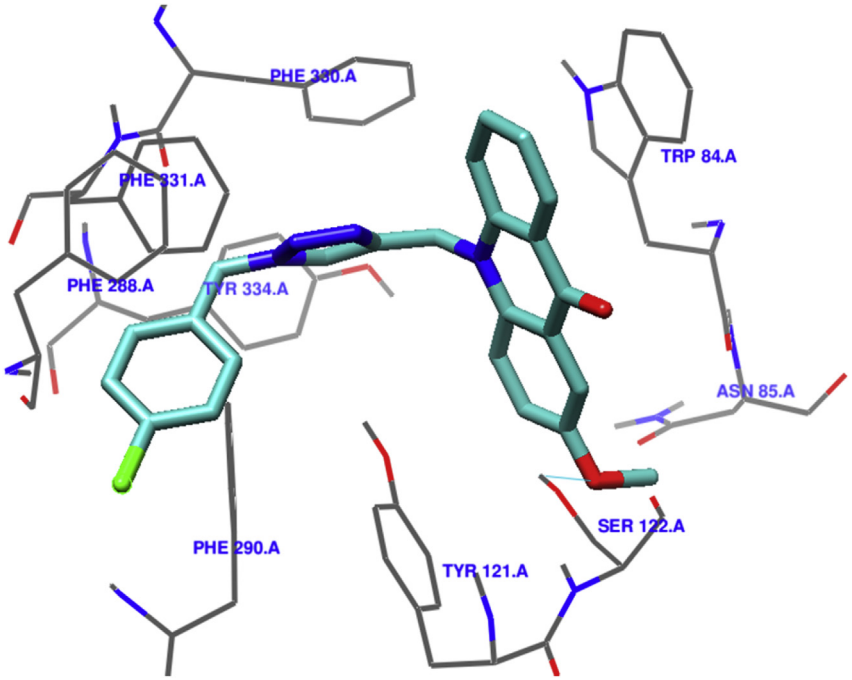

Fig. 3. Hydrogen bond between methoxy group and Ser122 in compound **9g**, constructed by UCSF package.

candidates.

3. Conclusion

In conclusion, various novel acridone linked to 1,2,3-triazole derivatives were designed, synthesized, and evaluated against AChE and BChE. Among them, 10-((1-(4-chlorobenzyl)-1*H*-1,2,3-triazol-4-yl)methyl)-1-methoxyacridin-9(10*H*)-one **9g** with IC_{50} value of 7.31 μM showed the best inhibitory activity against AChE. The docking study of compound **9g** with AChE enzyme showed that there is an appropriate CAS-ligand hydrogen binding interaction through methoxy group at 4-position of acridone and chlorine on the pendant benzyl group as well as π–π stacking interaction of acridone and 1,2,3-triazole rings. All these results clearly confirmed the efficacy of the corresponding compounds for further drug discovery developments.

4. Experimental

Melting points were measured with a Kofler hot stage apparatus and are uncorrected. ^{1}H and ^{13}C NMR spectra were recorded with a Bruker FT-400, using TMS as an internal standard. IR spectra were obtained with a Nicolet Magna FTIR 550 spectrophotometer (KBr disks). MS were recorded with an Agilent Technology (HP) mass spectrometer operating at an ionization potential of 70 eV. Elemental analysis was performed with an Elementar Analysen system GmbH VarioEL CHNS mode.

4.1. General procedure for the synthesis of 2-arylamino benzoic acids ***3***

A solution of 2-bromobenzoic acid **1** (8.5 mmol), aniline derivative **2** (159.0 mmol), copper powder (4.7 mmol), and potassium

carbonate (119.0 mmol) in ethanol (80 ml) was heated at reflux for 7 h. After completion of reaction (checked by TLC), the reaction mixture was cooled down to room temperature, poured into hot water (1 l) and boiled in the presence of activated charcoal for 15 min. Then, it was filtered through celite and the filtrate was acidified with HCl to obtain precipitated product which was purified using recrystallization from ethanol to obtain pure products in 80–85% yield.

4.2. General procedure for the synthesis of acridone derivatives **4**

A mixture of 2-arylamino benzoic acids **3** (1 mmol) and polyphosphoric acid (10 mmol) was heated at 100 °C for 3 h. The reaction run to completion when brown color of the reaction mixture faded to yellow. Then, it was poured into hot water (500 ml) and made alkaline by liquor ammonia. Then, the obtained yellow precipitate was filtered off, washed with hot water, and purified using recrystallization from acetic acid to obtain pure products in 80–85% yield.

4.3. General procedure for the synthesis of 10-(prop-2-yn-1-yl) acridin-9-one derivatives **6**

A suspension of acridone derivative **4** (2.5 mmol) and potassium *tert*-butoxide (3.6 mmol) in DMSO (1.5 ml) was stirred at room temperature for 30 min. Then, it was added to a solution of propargyl bromide **5** (3.4 mmol) in DMSO (5 ml) drop wise and the reaction mixture was stirred at room temperature for 3 h. After that it was poured into crushed ice and the aqueous solution was extracted with dichloromethane (3 × 20 ml), washed with water, and dried over Na_2SO_4. The solvent was evaporated under vacuum and the residue was purified by flash chromatography on silica gel using petroleum ether/ethyl acetate (9:1) to obtain pure products in 55–70% yield.

4.4. General procedure for the synthesis of ocridone linked 1,2,3-triazole derivatives **9**

At first, azide derivatives **8** were prepared *in situ*. For this purpose, a solution of benzyl bromide derivative **7** (1.1 mmol), sodium azide (0.9 mmol), and Et_3N (1.3 mmol) in the mixture of water (4 ml)/*t*-BuOH (4 ml) was stirred at room temperature for 1 h. Subsequently, mixture of 10-(prop-2-yn-1-yl)acridin-9-one derivative **6** (1 mmol) and CuI (7 mol %) was added to the freshly prepared azide derivative **8** and the reaction mixture was stirred at room temperature for 24–56 h. Upon completion of the reaction, monitored by thin-layer chromatography, the reaction mixture was diluted with water, poured into crushed ice, and the precipitated product was filtered off, washed with cold water, and purified by flash chromatography on silica gel using petroleum ether/ethyl acetate (4:1).

4.4.1. 10-((1-Benzyl-1H-1,2,3-triazol-4-yl)methyl)acridin-9(10H)-one (**9a**)

Yellow crystals; yield: 85%, mp 215–217 °C. IR (KBr): 3123, 3071, 2925, 2852, 1732, 1632, 1598 cm^{-1}. ^1H NMR (400 MHz, DMSO-d_6): 8.36 (dd, J = 8.0, 1.6 Hz, 2H, H_1, H_8), 8.23 (s, 1H, triazole), 7.95 (d, J = 8.0 Hz, 2H, H_4, H_5), 7.81 (td, J = 8.0, 1.6 Hz, 2H, H_3, H_6), 7.37–7.30 (m, 5H, Ph), 7.27–7.25 (m, 2H, H_2, H_7), 5.81 (s, 2H, CH_2), 5.54 (s, 2H, CH_2). ^{13}C NMR (100 MHz, DMSO-d_6): 177.1, 143.2, 142.3, 136.4, 134.6, 129.2, 128.6, 128.3, 127.1, 124.0, 122.2, 122.0, 116.8, 53.3, 42.1. Anal. Calcd for $C_{23}H_{18}N_4O$: C, 75.39; H, 4.95; N, 15.29. Found: C, 75.58; H, 5.18; N, 15.08.

4.4.2. 10-((1-(4-Chlorobenzyl)-1H-1,2,3-triazol-4-yl)methyl) acridin-9(10H)-one (**9b**)

Pale yellow crystals; yield: 86%, mp > 250 °C. IR (KBr): 3099, 2924, 1730, 1630, 1598 cm^{-1}. ^1H NMR (400 MHz, DMSO-d_6): 8.36 (dd, J = 8.0, 1.6 Hz, 2H, H_1, H_8), 8.23 (s, 1H, triazole), 7.94 (d, J = 8.0 Hz, 2H, H_4, H_5), 7.82 (td, J = 8.0, 1.6 Hz, 2H, H_3, H_6), 7.41 (d, J = 8.8 Hz, 2H, $H_{3'}$, $H_{5'}$), 7.35 (t, J = 8.0 Hz, 2H, H_2, H_7), 7.29 (d, J = 8.8 Hz, 2H, $H_{2'}$, $H_{6'}$), 5.80 (s, 2H, CH_2), 5.54 (s, 2H, CH_2). ^{13}C NMR (100 MHz, DMSO-d_6): 177.1, 143.3, 142.3, 135.4, 134.7, 133.3, 130.3, 129.2, 127.1, 124.0, 122.2, 122.0, 116.8, 52.5, 42.1. Anal. Calcd for $C_{23}H_{17}ClN_4O$: C, 68.91; H, 4.27; N, 13.98. Found: C, 69.18; H, 4.43; N, 14.21.

4.4.3. 10-((1-Benzyl-1H-1,2,3-triazol-4-yl)methyl)-2-chloroacridin-9(10H)-one (**9c**)

Yellow crystals; yield: 83%, mp 241–242 °C. IR (KBr): 3080, 2919, 2855, 1732, 1635, 1598 cm^{-1}. ^1H NMR (400 MHz, DMSO-d_6): 8.36 (d, J = 8.0 Hz, 1H, H_8), 8.26 (s, 1H, H_1), 8.22 (s, 1H, triazole), 8.02 (d, J = 9.0 Hz, 1H, H_3), 7.96 (d, J = 9.0 Hz, 1H, H_4), 7.85–7.83 (m, 2H, H_5, H_6), 7.40–7.25 (m, 6H, Ph, H_7), 5.81 (s, 2H, CH_2), 5.54 (s, 2H, CH_2). ^{13}C NMR (100 MHz, DMSO-d_6): 176.1, 142.9, 142.1, 141.0, 136.4, 135.0, 134.3, 129.2, 128.6, 128.3, 127.1, 126.6, 125.7, 124.0, 123.0, 122.4, 122.0, 119.6, 116.9, 53.3, 42.3. Anal. Calcd for $C_{23}H_{17}ClN_4O$: C, 68.91; H, 4.27; N, 13.98. Found: C, 68.81; H, 4.12; N, 14.16.

4.4.4. 2-Chloro-10-((1-(4-chlorobenzyl)-1H-1,2,3-triazol-4-yl) methyl)acridin-9(10H)-one (**9d**)

Yellow crystals; yield: 79%, mp 243–245 °C. IR (KBr): 3102, 2957, 2855, 1745, 1626, 1595, 1492 cm^{-1}. ^1H NMR (400 MHz, DMSO-d_6): 8.35 (d, J = 8.0 Hz, 1H, H_8), 8.26 (s, 1H, H_1), 8.22 (s, 1H, triazole), 8.02 (d, J = 8.5 Hz, 1H, H_3), 7.96 (d, J = 8.5 Hz, 1H, H_4), 7.85–7.83 (m, 2H, H_5, H_6), 7.43–7.28 (m, 5H, H_7, $H_{2'}$, $H_{3'}$, $H_{5'}$, $H_{6'}$), 5.81 (s, 2H, CH_2), 5.54 (s, 2H, CH_2). ^{13}C NMR (100 MHz, DMSO-d_6): 176.1, 143.0, 142.2, 141.0, 135.3, 135.0, 134.3, 133.3, 130.3, 129.2, 127.1, 126.6, 125.7, 124.1, 123.0, 122.5, 122.0, 119.6, 116.9, 52.5, 42.3. MS m/z (%) 438 ([$M^{+\bullet}$[4+, 436 ,(1 ([$M^{+\bullet}$+2]434 ,(6 , ($M^{+\bullet}$, 10), 393 (86), 364 (22), 302 (41), 274 (17), 258 (27), 174 (50), 91 (100). Anal. Calcd for $C_{23}H_{16}Cl_2N_4O$: C, 63.46; H, 3.70; N, 12.87. Found: C, 63.31; H, 3.85; N, 12.67.

4.4.5. 2-Chloro-10-((1-(4-nitrobenzyl)-1H-1,2,3-triazol-4-yl) methyl)acridin-9(10H)-one (**9e**)

Yellow crystals; yield: 73%, mp > 250 °C. IR (KBr): 2927, 2842, 1735, 1627, 1594, 1522, 1352 cm^{-1}. ^1H NMR (400 MHz, DMSO-d_6): 8.35 (dd, J = 8.0, 1.6 Hz, 1H, H_8), 8.28 (s, 1H, H_1), 8.27 (s, 1H, triazole), 8.21 (d, J = 8.8 Hz, 2H, $H_{3'}$, $H_{5'}$), 8.02 (d, J = 9.0 Hz, 1H, H_3), 7.96 (d, J = 9.0 Hz, 1H, H_4), 7.87–7.84 (m, 2H, H_5, H_6), 7.48 (d, J = 8.8 Hz, 2H, $H_{2'}$, $H_{6'}$), 7.39 (t, J = 8.0 Hz, 1H, H_7), 5.84 (s, 2H, CH_2), 5.72 (s, 2H, CH_2). ^{13}C NMR (100 MHz, DMSO-d_6): 176.1, 147.8, 143.7, 143.1, 142.1, 140.9, 135.1, 134.4, 129.5, 127.2, 126.7, 125.7, 124.5, 124.3, 123.1, 122.5, 122.1, 119.6, 116.9, 52.4, 42.3. Anal. Calcd for $C_{23}H_{16}ClN_5O_3$: C, 61.96; H, 3.62; N, 15.71. Found: C, 62.14; H, 3.48; N, 15.55.

4.4.6. 10-((1-Benzyl-1H-1,2,3-triazol-4-yl)methyl)-2-methoxyacridin-9(10H)-one (**9f**)

Yellow crystals; yield: 85%, mp 196–197 °C. IR (KBr): 3070, 2923, 2853, 1745, 1630, 1596, 1503 cm^{-1}. ^1H NMR (400 MHz, DMSO-d_6): 8.35 (d, J = 9.2 Hz, 1H, H_8), 8.18 (s, 1H, triazole), 7.96–7.92 (m, 2H, H_4, H_5), 7.80–7.76 (m, 2H, H_1, H_6), 7.46 (dd, J = 9.4, 3.0 Hz, 1H, H_3), 7.35–724 (m, 6H, Ph, H_7), 5.80 (s, 2H, CH_2), 5.53 (s, 2H, CH_2), 3.37 (s, 3H, OCH_3). ^{13}C NMR (100 MHz, DMSO-d_6): 176.5, 154.6, 143.3, 141.8, 137.0, 136.4, 134.3, 129.2, 128.6, 128.3, 127.1, 124.4, 123.9, 122.9, 121.6, 121.4, 118.8, 116.6, 106.6, 55.9, 53.2, 42.1. Anal. Calcd for $C_{24}H_{20}N_4O_2$: C, 72.71; H, 5.09; N, 14.13. Found: C, 72.60; H, 4.85; N, 13.90.

*4.4.7. 10-((1-(4-Chlorobenzyl)-1H-1,2,3-triazol-4-yl)methyl)-2-methoxyacridin-9(10H)-one (**9g**)*

Deep yellow crystals; yield: 84%, mp 199–200 °C. IR (KBr): 2923, 2852, 1742, 1630, 1597, 1497 cm^{-1}. ^1H NMR (400 MHz, DMSO-d_6): 8.36 (dd, J = 7.7, 1.6 Hz, 1H, H_8), 8.17 (s, 1H, triazole), 7.96–7.92 (m, 2H, H_4, H_5), 7.80 (td, J = 7.7, 1.6 Hz, 1H, H_6), 7.77 (d, J = 3.0 Hz, 1H, H_1), 7.46 (dd, J = 9.4, 3.0 Hz, 1H, H_3), 7.41 (d, J = 8.4 Hz, 2H, $H_{3'}$, $H_{5'}$), 7.33 (t, J = 7.7 Hz, 1H, H_7), 7.28 (d, J = 8.4 Hz, 2H, $H_{2'}$, $H_{6'}$), 5.80 (s, 2H, CH_2), 5.36 (s, 2H, CH_2), 3.37 (s, 3H, OCH_3). ^{13}C NMR (100 MHz, DMSO-d_6): 176.0, 154.3, 143.5, 137.1, 135.5, 134.3, 130.3, 129.2, 127.2, 124.4, 124.0, 122.5, 122.7, 122.8, 121.7, 111.5, 118.8, 116.6, 106.1, 56.3, 53.1, 43.0. Anal. Calcd for $C_{24}H_{19}ClN_4O_2$: C, 66.90; H, 4.44; N, 13.00. Found: C, 67.11; H, 4.58; N, 12.87.

*4.4.8. 10-((1-Benzyl-1H-1,2,3-triazol-4-yl)methyl)-2-bromoacridin-9(10H)-one (**9h**)*

Yellow crystals; yield: 78%, mp 248–249 °C. IR (KBr): 3077, 2925, 2855, 1732, 1629, 1598, 1492 cm^{-1}. ^1H NMR (400 MHz, DMSO-d_6): 8.40 (s, 1H, H_1), 8.34 (d, J = 8.0 Hz, 1H, H_8), 8.21 (s, 1H, triazole), 7.96–7.94 (m, 3H, H_3, H_4, H_5), 7.83 (t, J = 8.0 Hz, 1H, H_6), 7.35–724 (m, 6H, Ph, H_7), 5.80 (s, 2H, CH_2), 5.53 (s, 2H, CH_2). ^{13}C NMR (100 MHz, DMSO-d_6): 176.0, 142.9, 142.1, 141.3, 136.9, 136.4, 135.0, 129.2, 129.0, 128.6, 128.3, 127.1, 124.0, 123.5, 122.5, 122.2, 119.8, 117.0, 114.0, 53.3, 42.2. Anal. Calcd for $C_{23}H_{17}BrN_4O$: C, 62.03; H, 3.85; N, 12.58. Found: C, 61.88; H, 3.72; N, 12.71.

*4.4.9. 2-Bromo-10-((1-(4-chlorobenzyl)-1H-1,2,3-triazol-4-yl)methyl)acridin-9(10H)-one (**9i**)*

Yellow crystals; yield: 74%, mp 250–251 °C. IR (KBr): 2924, 2851, 1730, 1630, 1597 cm^{-1}. ^1H NMR (400 MHz, DMSO-d_6): 8.41 (t, J = 1.6 Hz, 1H, H_1), 8.35 (dd, J = 8.0, 1.6 Hz, 1H, H_8), 8.21 (s, 1H, triazole), 7.96–7.94 (m, 3H, H_3, H_4, H_5), 7.84 (td, J = 8.0, 1.6 Hz, 1H, H_6), 7.43 (d, J = 8.4 Hz, 2H, $H_{3'}$, $H_{5'}$), 7.37 (t, J = 8.0 Hz, 1H, H_7), 7.30 (d, J = 8.4 Hz, 2H, $H_{2'}$, $H_{6'}$), 5.81 (s, 2H, CH_2), 5.54 (s, 2H, CH_2). ^{13}C NMR (100 MHz, DMSO-d_6): 176.1, 143.0, 142.1, 141.3, 137.0, 135.6, 135.1, 133.2, 130.3, 129.2, 128.5, 128.9, 127.2, 124.1, 123.5, 122.5, 119.8, 117.0, 114.4, 52.5, 42.2. Anal. Calcd for $C_{23}H_{16}BrClN_4O$: C, 57.58; H, 3.36; N, 11.68. Found: C, 57.36; H, 3.48; N, 11.82.

*4.4.10. 2-Bromo-10-((1-(4-nitrobenzyl)-1H-1,2,3-triazol-4-yl)methyl)acridin-9(10H)-one (**9j**)*

Yellow crystals; yield: 68%, mp > 250 °C. IR (KBr): 2923, 2853, 1741, 1624, 1594, 1521, 1350 cm^{-1}. ^1H NMR (400 MHz, DMSO-d_6): 8.41 (t, J = 1.6 Hz, 1H, H_1), 8.35 (dd, J = 8.0, 1.6 Hz, 1H, H_8), 8.27 (s, 1H, triazole), 8.21 (d, J = 8.8 Hz, 2H, $H_{3'}$, $H_{5'}$), 7.98–7.96 (m, 3H, H_3, H_4, H_5), 7.85 (td, J = 8.0, 1.6 Hz, 1H, H_6), 7.39 (d, J = 8.8 Hz, 2H, $H_{2'}$, $H_{6'}$), 7.37 (t, J = 8.0 Hz, 1H, H_7), 5.84 (s, 2H, CH_2), 5.72 (s, 2H, CH_2). ^{13}C NMR (100 MHz, DMSO-d_6): 175.8, 143.4, 143.2, 142.2, 140.5, 137.4, 131.5, 129.5, 128.7, 128.1, 126.5, 125.3, 124.3, 123.0, 122.4, 122.3, 120.8, 116.8, 114.5, 53.1, 42.1. Anal. Calcd for $C_{23}H_{16}BrN_5O_3$: C, 56.34; H, 3.29; N, 14.28. Found: C, 56.14; H, 3.11; N, 14.51.

*4.4.11. 10-((1-Benzyl-1H-1,2,3-triazol-4-yl)methyl)-2-methylacridin-9(10H)-one (**9k**)*

Pale yellow crystals; yield: 89%, mp 231–232 °C. IR (KBr): 3127, 2922, 2854, 1730, 1634, 1597, 1485 cm^{-1}. ^1H NMR (400 MHz, DMSO-d_6): 8.35 (dd, J = 8.0, 1.6 Hz, 1H, H_8), 8.17 (s, 1H, triazole), 8.15 (d, J = 1.5 Hz, 1H, H_1), 7.92 (d, J = 8.0 Hz, 1H, H_5), 7.87 (d, J = 8.8 Hz, 1H, H_4), 7.79 (td, J = 8.0, 1.6 Hz, 1H, H_6), 7.64 (dd, J = 8.8, 1.5 Hz, 1H, H_3), 7.35–725 (m, 6H, Ph, H_7), 5.78 (s, 2H, CH_2), 5.53 (s, 2H, CH_2), 2.44 (s, 3H, CH_3). ^{13}C NMR (100 MHz, DMSO-d_6): 176.9, 143.3, 142.1, 140.4, 136.4, 136.0, 134.5, 131.2, 129.3, 129.2, 128.6, 128.3, 127.1, 126.3, 123.9, 122.1, 121.7, 116.8, 116.6, 53.2, 42.0, 20.7. Anal. Calcd for $C_{24}H_{20}N_4O$: C, 75.77; H, 5.30; N, 14.73. Found: C, 75.91; H, 5.17; N, 14.50.

*4.4.12. 10-((1-(4-Chlorobenzyl)-1H-1,2,3-triazol-4-yl)methyl)-2-methylacridin-9(10H)-one (**9l**)*

Yellow crystals; yield: 78%, mp > 250 °C. IR (KBr): 3050, 2923, 2852, 1735, 1612, 1593 cm^{-1}. ^1H NMR (400 MHz, DMSO-d_6): 8.35 (d, J = 7.5 Hz, 1H, H_8), 8.17 (s, 1H, triazole), 8.15 (s, 1H, H_1), 7.91 (d, J = 7.5 Hz, 1H, H_5), 7.85 (d, J = 8.5 Hz, 1H, H_4), 7.79 (t, J = 7.5 Hz, 1H, H_6), 7.64 (d, J = 8.5 Hz, 1H, H_3), 7.41 (d, J = 8.4 Hz, 2H, $H_{3'}$, $H_{5'}$), 7.32 (t, J = 7.5 Hz, 1H, H_7), 7.28 (d, J = 8.4 Hz, 2H, $H_{2'}$, $H_{6'}$), 5.78 (s, 2H, CH_2), 5.58 (s, 2H, CH_2), 2.43 (s, 3H, CH_3). ^{13}C NMR (100 MHz, DMSO-d_6): 176.1, 143.4, 142.1, 140.4, 136.0, 135.4, 133.3, 131.2, 130.3, 129.3, 129.2, 127.2, 127.1, 126.3, 123.9, 122.1, 121.7, 116.8, 116.6, 52.4, 42.0, 20.6. MS m/z (%) 416 ([$M^{+\bullet}$+2]414 ,(1 , ($M^{+\bullet}$, 3), 486 (22), 471 (30), 425 (16), 401 (28), 379 (18), 358 (20), 324 (26), 231 (20), 215 (73), 188 (43), 159 (40), 174 (100), 132 (98), 105 (33), 91 (99), 77 (87). Anal. Calcd for $C_{24}H_{19}ClN_4O$: C, 69.48; H, 4.62; N, 13.50. Found: C, 69.31; H, 4.49; N, 13.68.

*4.4.13. 10-((1-Benzyl-1H-1,2,3-triazol-4-yl)methyl)-4-fluoroacridin-9(10H)-one (**9m**)*

White crystals; yield: 87%, mp 182–184 °C. IR (KBr): 3147, 2928, 1730, 1635, 1605 cm^{-1}. ^1H NMR (400 MHz, DMSO-d_6): 8.30 (d, J = 7.6 Hz, 1H, H_8), 8.20 (s, 1H, triazole), 8.19 (d, J = 8.0 Hz, 1H, H_1), 7.82–7.81 (m, 2H, H_5, H_6), 7.69 (dd, J = 15.4, 7.6 Hz, 1H, H_3), 7.38–7.31 (m, 5H, Ph), 7.25–7.23 (m, 2H, H_2, H_7), 5.71 (s, 2H, CH_2), 5.56 (s, 2H, CH_2). ^{13}C NMR (100 MHz, DMSO-d_6): 176.7, 151.5 (d, $J_{C\text{-}F}$ = 245.0 Hz), 144.7, 144.0, 136.5, 135.0, 129.2, 128.5, 128.2, 126.9, 125.4, 123.8 (d, $J_{C\text{-}F}$ = 4.2 Hz), 123.2 (d, $J_{C\text{-}F}$ = 3.6 Hz), 122.7, 122.4 (d, $J_{C\text{-}F}$ = 8.3 Hz), 122.3, 121.7, 121.5, 117.2, 53.2, 47.6 (d, $J_{C\text{-}F}$ = 14.7 Hz). Anal. Calcd for $C_{23}H_{17}FN_4O$: C, 71.86; H, 4.46; N, 14.57. Found: C, 71.70; H, 4.32; N, 14.68.

*4.4.14. 10-((1-(4-Chlorobenzyl)-1H-1,2,3-triazol-4-yl)methyl)-4-fluoroacridin-9(10H)-one (**9n**)*

White crystals; yield: 88%, mp 208–209 °C. IR (KBr): 3154, 2923, 1735, 1637, 1607 cm^{-1}. ^1H NMR (400 MHz, DMSO-d_6): 8.30 (d, J = 8.3 Hz, 1H, H_8), 8.22 (s, 1H, triazole), 8.19 (d, J = 7.5 Hz, 1H, H_1), 7.81–7.80 (m, 2H, H_5, H_6), 7.68 (ddd, J = 15.5, 7.5, 1.6 Hz, 1H, H_3), 7.41 (d, J = 8.4 Hz, 2H, $H_{3'}$, $H_{5'}$), 7.38–7.31 (m, 2H, H_2, H_7), 7.28 (d, J = 8.4 Hz, 2H, $H_{2'}$, $H_{6'}$), 5.71 (s, 2H, CH_2), 5.57 (s, 2H, CH_2). ^{13}C NMR (100 MHz, DMSO-d_6): 176.5, 151.8 (d, $J_{C\text{-}F}$ = 245.1 Hz), 144.8, 144.0, 135.5, 135.0, 133.3, 132.6 (d, $J_{C\text{-}F}$ = 5.9 Hz), 130.2, 129.2, 126.9, 125.4, 123.8 (d, $J_{C\text{-}F}$ = 4.3 Hz), 123.2 (d, $J_{C\text{-}F}$ = 3.0 Hz), 122.7, 122.4 (d, $J_{C\text{-}F}$ = 8.4 Hz), 121.7, 121.5, 117.2, 52.5, 47.6 (d, $J_{C\text{-}F}$ = 15.0 Hz). Anal. Calcd for $C_{23}H_{16}ClFN_4O$: C, 65.95; H, 3.85; N, 13.38. Found: C, 66.15; H, 3.94; N, 13.12.

4.5. AChE and BChE inhibition assay

Acetylcholinesterase (AChE, E.C. 3.1.1.7, Type V-S, lyophilized powder, from electric eel, 1000 unit), butylcholinesterase (BChE, E.C. 3.1.1.8, from equine serum), acetylthiocholine iodide (ATCI), and 5,5-dithiobis-(2-nitrobenzoic acid) (DTNB) were purchased from Sigma–Aldrich. Potassium dihydrogen phosphate, dipotassium hydrogen phosphate, potassium hydroxide, and sodium hydrogen carbonate were obtained from Fluka. The solutions of the title compounds were prepared in a mixture of DMSO (5 ml) and methanol (5 ml) and diluted in 0.1 M KH_2PO_4/K_2HPO_4 buffer (pH 8.0) to obtain final assay concentrations. All experiments were achieved at 25 °C. Six different concentrations were tested for each compound in triplicate to obtain the range of 20%–80% inhibition for AChE.

To measure *in vitro* AChE activity, modified Ellman's method was performed [27] using a 96-well plate reader (BioTek ELx808). Each well contained 50 μl potassium phosphate buffer (KH_2PO_4/K_2HPO_4, 0.1 M, pH 8), 25 μl sample dissolved in 50% methanol and 50%

DMSO and 25 μl enzyme (final concentration 0.22 U/ml in buffer). They were preincubated for 15 min at room temperature, then 125 μl DTNB (3 mM in buffer) was added. Characterization of the hydrolysis of ATCI catalyzed by AChE was performed spectrometrically at 405 nm followed by the addition of substrate (ATCI 3 mM in water). The change in absorbance was measured at 405 nm after 15 min. The IC_{50} values were determined graphically from inhibition curves (log inhibitor concentration vs. percent of inhibition). A control experiment was performed under the same conditions without inhibitor and the blank contained buffer, water, DTNB, and substrate. The described method was also used for BChE inhibition assay.

4.6. DPPH radical scavenging activity (DPPH)

Antioxidant activity of compounds **9b**, **9c**, **9f**, **9k**, and **9m** were assessed using DPPH (1,1-diphenyl-2-picrylhydrazyl) [30]. Several concentrations of test compounds in DMSO were prepared. The compound solution (0.5 ml) was added to the methanolic DPPH solution (1.0 ml, 0.1 mM), and the mixture was kept in the dark for 30 min. Then, the absorbance at 517 nm was measured by an UV/visible spectrophotometer. The percent scavenging activity was calculated using the following formula: inhibition $(\%) = 100 - [100 \times (Abs_{sample} - Abs_{control})/Abs_{blank}]$.

4.7. Molecular docking study

Docking studies were carried out using the AUTODOCK 4.2 program. For this purpose, the pdb structure of 1EVE was taken from the Brookhaven protein database (http://www.rcsb.org) as a complex bound with inhibitor E2020 (donepezil). Subsequently, the water molecules and the original inhibitors were removed from the protein structure. The 3D structure of the compound **9g** was provided using MarvineSketch 5.8.3, 2012, ChemAxon (http://www.chemaxon.com) and converted to pdbqt coordinate by AUTODOCK 4.2 program. Also, the autodock format of protein was provided using the same software. Polar hydrogen atoms were added to amino acid residues using Autodock Tools (ADT; version 1.5.6), Koullman charges were assigned to all atoms of the enzyme, and the obtained enzyme structure was used as an input for the AUTOGRID program. AUTOGRID performed a pre calculated atomic affinity grid maps for each atom type in the ligand, plus an electrostatics map and a separate desolation map presented in the substrate molecule. All maps were calculated with 0.375 Å spacing between grid points. The center of the grid box was placed at the center of donepezil with coordinates x = 2.023, y = 63.295, z = 67.062. The dimensions of the active site box were set at 40 × 40 × 40 × A. Flexible ligand docking was accomplished for the compound **9g**. Each docked system was carried out by 100 runs of the AUTODOCK search by the Lamarckian genetic algorithm (LGA). Other than the above mentioned parameters, the other parameters were accepted as default. The lowest energy conformation of ligand–enzyme complex was considered for analyzing the interactions between AChE and the inhibitor. The results were visualized using Discovery Studio 4.0 Client (Figs. 1 and 2) and Chimera 1.9 (Fig. 3) (Molecular graphics and analyses were performed with the UCSF Chimera package. Chimera is developed by the Resource for Biocomputing, Visualization, and Informatics at the University of California, San Francisco).

4.8. Computational methods

The log P values and tPSA were calculated using the ChemDraw Ultra 12.0 [33]. The polar surface area (tPSA) was calculated by the atom-based method. HBD and HBA were calculated by the means of MarvineSketch 5.8.3. RBC was calculated using Autodock Tools (ver. 1.5.4).

Acknowledgments

This work was supported by grants from the Research Council of Tehran University of Medical Sciences.

Appendix A. Supplementary data

Supplementary data related to this article can be found at http://dx.doi.org/10.1016/j.ejmech.2015.01.044.

References

[1] N.C. Berchtold, C.W. Cotman, Evolution in the conceptualization of dementia and Alzheimer's disease: Greco-Roman period to the 1960s, Neurobiol. Aging 19 (1998) 173–189.
[2] C. Ballard, S. Gauthier, A. Corbett, C. Brayne, D. Aarsland, E. Jones, Alzheimer's diseases, Lancet 377 (2011) 1019–1031.
[3] C. Mount, C. Downton, Alzheimer disease: progress or profit, Nat. Med. 12 (2006) 780–784.
[4] R.E. Becker, N.H. Greig, E. Giacobini, L.S. Schneider, L. Ferrucci, A new roadmap for drug development for Alzheimer's disease, Nat. Rev. Drug Discov. 13 (2014) 156.
[5] F. Mao, L. Huang, Z. Luo, A. Liu, C. Lu, Z. Xie, X. Li, *O*-Hydroxyl- or o-amino benzylamine-tacrine hybrids: multifunctional biometals chelators, antioxidants, and inhibitors of cholinesterase activity and amyloid-β aggregation, Bioorg. Med. Chem. 20 (2012) 5884–5892.
[6] X. Zhou, X.-B. Wang, T. Wang, L.-Y. Kong, Design, synthesis, and acetylcholinesterase inhibitory activity of novel coumarin analogues, Bioorg. Med. Chem. 16 (2008) 8011–8021.
[7] H. Tang, H.-T. Zhao, S.-M. Zhong, Z.-Y. Wang, Z.-F. Chen, H. Liang, Novel oxoisoaporphine-based inhibitors of acetyl- and butyrylcholinesterase and acetylcholinesterase-induced beta-amyloid aggregation, Bioorg. Med. Chem. Lett. 22 (2012) 2257–2261.
[8] M.L. Bolognesi, A. Cavalli, L. Valgimigli, M. Bartolini, M. Rosini, V. Andrisano, M. Recanatini, C. Melchiorre, Multi-target-directed drug design strategy: from a dual binding site acetylcholinesterase inhibitor to a trifunctional compound against Alzheimer's disease, J. Med. Chem. 50 (2007) 6446–6449.
[9] Y. Miyamae, M. Kurisu, K. Murakami, J. Han, H. Isoda, K. Irie, H. Shigemori, Protective effects of caffeoylquinic acids on the aggregation and neurotoxicity of the 42-residue amyloid β-protein, Bioorg. Med. Chem. 20 (2012) 5844.
[10] E. Scarpini, P. Scheltens, H. Feldman, Treatment of Alzheimer's disease; current status and new perspectives, Lancet Neurol. 2 (2003) 539–547.
[11] A. Chatonnet, O. Lockridge, Comparison of butyrylcholinesterase and acetylcholinesterase, Biochem. J. 260 (1989) 625–634.
[12] K.A. Carson, C. Geula, M.-M. Mesulam, Electron microscopic localization of cholinesterase activity in Alzheimer brain tissue, Brain Res. 540 (1991) 204–208.
[13] L.S. Schneider, A critical review of cholinesterase inhibitors as a treatment modality in Alzheimer's disease, Dialogues Clin. Neurosci. 2 (2000) 111–128.
[14] M.-K. Hu, L.-J. Wu, G. Hsiao, M.-H. Yen, Homodimeric tacrine congeners as acetylcholinesterase inhibitors, J. Med. Chem. 45 (2002) 2277–2282.
[15] P. Szymański, M. Markowicz, E. Mikiciuk-Olasik, Synthesis and biological activity of derivatives of tetrahydroacridine as acetylcholinesterase inhibitors, Bioorg. Chem. 39 (2011) 138–142.
[16] L. Fang, S. Jumpertz, Y. Zhang, D. Appenroth, C. Fleck, K. Mohr, C. Tränkle, M. Decker, Hybrid molecules from xanomeline and tacrine: enhanced tacrine actions on cholinesterases and muscarinic M1 receptors, J. Med. Chem. 53 (2010) 2094–2103.
[17] Y.Y. Yang, W. Yang, W.J. Zuo, Y.B. Zeng, S.B. Liu, W.L. Mei, H.F. Dai, Two new acridone alkaloids from the branch of Atalantia buxifolia and their biological activity, J. Asian Nat. Prod. Res. 15 (2013) 899–904.
[18] X.L. Zhu, N.X. Yu, G.F. Hao, W.C. Yang, G.F. Yang, Structural basis of femtomolar inhibitors for acetylcholinesterase subtype selectivity: insights from computational simulations, J. Mol. Graph. Model. 41 (2013) 55–60.
[19] W.G. Lewis, L.G. Green, F. Grynszpan, Z. Radić, P.R. Carlier, P. Taylor, M.G. Finn, K.B. Sharpless, Click chemistry in situ: acetylcholinesterase as a reaction vessel for the selective assembly of a femtomolar inhibitor from an array of building blocks, Angew. Chem. Int. Ed. Engl. 41 (2002) 1053–1057.
[20] S. Senapati, Y. Cheng, J.A. McCammon, In-situ synthesis of a tacrine-triazole-based inhibitor of acetylcholinesterase: configurational selection imposed by steric interactions, J. Med. Chem. 49 (2006) 6222–6230.
[21] H. Akrami, B.F. Mirjalili, M. Khoobi, H. Nadri, A. Moradi, A. Sakhteman, S. Emami, A. Foroumadi, A. Shafiee, Indolinone-based acetylcholinesterase inhibitors: synthesis, biological activity and molecular modeling, Eur. J. Med. Chem. 84 (2014) 375–381.
[22] M. Khoobi, M. Alipour, A. Sakhteman, H. Nadri, A. Moradi, M. Ghandi, S. Emami, A. Foroumadi, A. Shafiee, Design, synthesis, biological evaluation

and docking study of 5-oxo-4,5-dihydropyrano[3,2-*c*]chromene derivatives as acetylcholinesterase and butyrylcholinesterase inhibitors, Eur. J. Med. Chem. 68 (2013) 260–269.
[23] A. Asadipour, M. Alipour, M. Jafari, M. Khoobi, S. Emami, H. Nadri, A. Sakhteman, A. Moradi, V. Sheibani, F.H. Moghadam, A. Shafiee, A. Foroumadi, Novel coumarin-3-carboxamides bearing *N*-benzylpiperidine moiety as potent acetylcholinesterase inhibitors, Eur. J. Med. Chem. 70 (2013) 623–630.
[24] C. Wolf, S. Liu, X. Mei, A.T. August, M. Casimir, Regioselective copper-catalyzed amination of bromobenzoic acids using aliphatic and aromatic amines, J. Org. Chem. 71 (2006) 3270–3273.
[25] R. Hedge, P. Thimmaiah, M.C. Yerigeri, G. Krishnegowda, K.N. Thimmaiah, P.J. Houghton, Anti-calmodulin acridone derivatives modulate vinblastine resistance in multidrug resistant (MDR) cancer cells, Eur. J. Med. Chem. 39 (2004) 161–178.
[26] H.C. Kolb, M.G. Finn, K.B. Sharpless, Click chemistry: diverse chemical function from a few good reactions, Angew. Chem. Int. Ed. 40 (2001) 2004–2021.
[27] G.L. Ellman, K.D. Courtney, V. Andres Jr., R.M. Feather-Stone, A new and rapid colorimetric determination of acetylcholinesterase activity, Biochem. Pharmacol. 7 (1961) 88–95.
[28] B. Kuhn, P. Mohr, M. Stahl, Intramolecular hydrogen bonding in medicinal chemistry, J. Med. Chem. 53 (2010) 2601–2611.
[29] C. Bissantz, B. Kuhn, M. Stahl, A medicinal chemist's guide to molecular interactions, J. Med. Chem. 53 (2010) 5061–5084.
[30] N. Yassa, H. Razavi Beni, A. Hadjiakhoondi, Free radical scavenging and lipid peroxidation activity of the Shahani black grape, Pak. J. Biol. Sci. 11 (2008) 2513–2516.
[31] C.A. Lipinski, F. Lombardo, B.W. Dominy, P.J. Feeney, Experimental and computational approaches to estimate solubility and permeability in drug discovery and development settings, Adv. Drug Deliv. Rev. 23 (1997) 3–25.
[32] C.A. Lipinski, Drug-like properties and the causes of poor solubility and poor permeability, J. Pharmacol. Toxicol. Methods 44 (2000) 235–249.
[33] ChemOffice, CambridgeSoftCorporation, Cambridge, USA, 2009.